Parity nonconservation in elastic $\vec{p}\,p$ scattering

C.-P. Liu,[1,*] C. H. Hyun,[2,3,†] and B. Desplanques[4,‡]
[1]*KVI, Zernikelaan 25, Groningen 9747 AA, The Netherlands*
[2]*Department of Physics, Seoul National University, Seoul, 151-742, Korea*
[3]*Institute of Basic Science, Sungkyunkwan University, Suwon 440-746, Korea*
[4]*Laboratoire de Physique Subatomique et de Cosmologie (UMR CNRS/IN2P3-UJF-INPG), F-38026 Grenoble Cedex, France*
(Received 12 December 2005; published 22 June 2006)

By looking at the parity-nonconserving (PNC) asymmetries for different energies in $\vec{p}\,p$ scattering, it is in principle possible to determine the PNC ρNN and ωNN couplings of a single-meson-exchange model of the PNC NN force. Analysis of the experimental data at 13.6, 45, and 221 MeV was performed by Carlson *et al.*, [Phys. Rev. C **65**, 035502 (2002)] who concluded the data were in agreement with the uncertainties accorded the original DDH estimates for the PNC meson-nucleon couplings. In this work it is shown first that a comparison with updated hadronic predictions of these couplings suggests the existence of some discrepancy for the PNC ωNN coupling. The effect of varying the strong coupling constants and introducing cutoffs in the one-boson-exchange weak potential is then investigated. As expected, the resulting asymmetry is quite sensitive to these parameters regardless of the energy. However, the above mentioned discrepancy persists. The dependence of this conclusion on various ingredients entering an improved description of the PNC NN force is also examined. Additional mechanisms include the two-pion resonance nature of the rho meson and some momentum dependence of the isoscalar PNC ρNN vertex. None of these corrections removes or even alleviates the above discrepancy. Their impact on the theoretical determination of the vector meson-nucleon couplings, the description of the PNC force in terms of single-meson exchange, and the interpretation of measurements are examined.

DOI: 10.1103/PhysRevC.73.065501 PACS number(s): 24.80.+y, 21.30.−x, 25.40.Cm

I. INTRODUCTION

It has been proposed that measurements of the parity-nonconserving (PNC) longitudinal asymmetry in $\vec{p}\,p$ scattering at different energies could provide a way to disentangle the separate contributions to the PNC NN force due to ρ- and ω-meson exchanges [1]. For some time, accurate measurements were available only at the low energies of 13.6 MeV [2] and 45 MeV [3]. Only recently a measurement, though less accurate, was finished at the higher energy of 221 MeV [4], which makes the above analysis possible. This task was done by Carlson *et al.* [5], who claimed that the results so obtained do not disagree with the largest range estimated by Desplanques, Donoghue, and Holstein (DDH) [6]. A rough understanding of the analysis is as follows. At the highest energy (221 MeV), where the contribution of the S to P NN states vanishes, the dominant contribution comes from the P to D transition. The corresponding ω-meson-exchange contribution is suppressed. As a result, this point allows one to fix the ρNN coupling, h_ρ^{pp}. Looking at the low-energy points, it is found that the ρ-exchange force so derived generates PNC asymmetries larger than those measured. Accounting for the experiments is accomplished by fitting the part of the force due to ω-meson exchange, which fixes the ωNN coupling, h_ω^{pp}. In the absence of experimental error, h_ω^{pp} appears to have a positive sign, opposite the negative sign of the DDH "best-guess" value, and a magnitude at the extreme limit of the DDH estimated range.

Besides the DDH work, there are many predictions for PNC meson-nucleon couplings in the literature. Most of them correspond to contributions already included in the DDH work (see Ref. [7] for references). Two updated ranges for the PNC couplings are given in Refs. [8,9], and they do not leave much room for a positive value of the ωNN coupling. This makes it more difficult to accommodate the value derived from the analysis by Carlson *et al.* [5]. Moreover, as especially noted by Feldman *et al.* [9], predictions for ρ and ω couplings are not independent of each other. According to this observation, a larger h_ω^{pp} would imply an h_ρ^{pp} algebraically larger than the DDH "best-guess" value, rather than smaller as found in the analysis by Carlson *et al.* [5]. An approach quite different from DDH was taken by Kaiser and Meissner [10], who used the chiral-soliton model. Their predictions differ from the "best-guess" values but nevertheless fit into the estimated range. Actually, they could be approximately obtained from the DDH work by weighting differently the various contributions considered there and taking into account the specific dependence of the coupling constants on the meson squared momentum, q^2. While the DDH estimates are, in principle, made at the meson mass ($q^2 = m^2$), Kaiser and Meissner's estimates are given at $q^2 = 0$. The momentum dependence, which was accounted for very roughly in the DDH work, has been looked at in detail by Kaiser and Meissner in their framework [11]. It is found to be especially important for the isoscalar PNC ρNN coupling.

From looking at the different hadronic predictions, it appears very unlikely that h_ω^{pp} can acquire a positive value. But, before jumping to the speculate about what could go

*Electronic address: liu@kvi.nl. Present address: T-16, Theoretical Division, Los Alamos National Laboratory, Los Alamos, NM 87545.
†Electronic address: hch@meson.skku.ac.kr
‡Electronic address: desplanq@lpsc.in2p3.fr

wrong in these hadronic calculations, it is important to check the analysis which depends quite sensitively on various issues in the two-nucleon dynamics. In the past, many of these issues have been surveyed by Simonius [1], Nessi-Tedaldi and Simonius [12], Driscoll and Miller [13,14], and Carlson *et al*. [5]. The aim of this current work is to study whether there is some missing two-nucleon dynamics, besides that considered previously, which could possibly restore h_ω^{pp} to more conventional values anticipated by existing hadronic calculations.

On the basis of the DDH "best-guess" values of meson-nucleon couplings, it is generally considered that the contribution to PNC effects in $\vec{p}p$ scattering is dominated by ρ-meson exchange. Although the contributions from ω-meson exchange are not negligible at low energy, they only constitute about a 20% or -30% correction, based on the DDH "best-guess" values or the fitted values by Carlson *et al*. It is therefore appropriate to concentrate on the ρ-meson-exchange contribution as a first step. Taking into account the uncertainty of the ρNN coupling, one can temporarily fix h_ρ^{pp} to reproduce the low-energy measurements, which are the most accurate. When this is done, it is found that the measured asymmetry at the highest energy point (221 MeV) is off by a factor of about 2. Therefore, any effect that could enhance the transition from P to D states (dominant for 221 MeV) with respect to the one from S to P states (dominant for 13.6 and 45 MeV) is of relevance for our purpose. Possibilities include: (1) a larger vector-meson tensor coupling κ_V [15], (2) hadronic form factors at the strong-interaction vertex, (3) the two-pion resonance nature of the rho meson [16] and (4) the momentum dependence of the weak meson-nucleon vertex [7,11]. For the last three cases, the enhancement can be naively expected from the resulting longer range of the PNC NN force, which generally favors transition amplitudes involving higher orbital angular momenta. However, it should be noted that the first and third cases may not be independent [15]. For the parity-conserving (PC) NN force, we use the AV18 model [17].

This paper is structured as follows. In Sec. II, the definition of the PNC longitudinal asymmetry and its analytic form are given. In Sec. III, we concentrate on the description of the PNC vector-meson-exchange potential, especially for the ρ-meson part. This involves standard variations of this potential but also less-known ones. We show in detail how the standard meson-exchange potential is extended to incorporate the 2π-exchange contribution and the form factor of the PNC vertex. The asymmetries resulting from different variations of two-nucleon dynamics are presented in Sec. IV. Their implications are discussed and new values of the weak couplings are obtained from a least-χ^2 fit to the measurements. The conclusion follows in Sec. V.

II. BASIC FORMALISM

The longitudinal asymmetry for nucleon scattering, with an incident energy E and a scattering angle θ, is defined as

$$A_L(E,\theta) = \frac{\sigma_+(E,\theta) - \sigma_-(E,\theta)}{\sigma_+(E,\theta) + \sigma_-(E,\theta)}, \tag{1}$$

where σ_+ and σ_- are differential cross sections for projectiles of positive and negative helicities, respectively. In theoretical analyses, however, it is the so-called "nuclear" total asymmetry, $A_L^{\rm tot}(E)$, that is often used [1,5,12,13,18,19]. For processes involving Coulomb interactions, such as $\vec{p}p$ scattering in this discussion, the total asymmetry is in fact ill-defined, because total cross sections diverge. The remedy is to remove the pure Coulomb contribution from the total cross section: by the optical theorem, the total cross section can be related to the forward scattering amplitude $\bar{f}(E,\theta=0)$ as

$$\sigma^{\rm tot} = \frac{4\pi}{k}{\rm Im}[\bar{f}(E,\theta=0)], \tag{2}$$

where k is the relative momentum. One can then subtract the pure Coulomb scattering amplitude f_C, which is singular at $\theta = 0$, and use the remaining regular "nuclear" scattering amplitude, $f = \bar{f} - f_C$, to define $A_L^{\rm tot}(E)$.

After the spin sums are carried out, the "nuclear" total asymmetry for $\vec{p}p$ scattering takes the following form:

$$A_L^{\rm tot}(E) = \frac{{\rm Im}[\tilde{f}_{10,00}(E,0) + \tilde{f}_{00,10}(E,0)]}{{\rm Im}\left[\sum_{S,M_S} f_{SM_S,SM_S}(E,0)\right]}, \tag{3}$$

where the subscripts $S'M'_S$, SM_S denote the final and initial two-body spin states, respectively. The notation $\tilde{f}$ is used to remind a PNC scattering amplitude: in order to maintain the Pauli principle for a pp system, a spin change must be accompanied by an orbital angular momentum change, that is, a parity change, too.

In this work, we treat the PNC interaction, V_{PNC}, as a perturbation. The unperturbed wave functions are solved numerically from the Lippmann-Schwinger equation

$$|\psi\rangle^{(\pm)} = |\phi\rangle^{(\pm)} + \frac{1}{E - H_0 - V_C \pm i\epsilon} V_S |\psi\rangle^{(\pm)}, \tag{4}$$

where V_C and V_S are the Coulomb and strong interactions, respectively; and $|\phi\rangle^{(\pm)}$ is the solution of Coulomb scattering.

The PC scattering amplitude is given by the following formula:

$$\begin{aligned} f_{S'M'_S,SM_S}(E,\theta) = \sqrt{4\pi}\sum_{JLL'} \sqrt{2L+1}\epsilon_{L'S'}\epsilon_{LS} \\ \times \langle L'(M_S - M'_S), S'M'_S | JM_S\rangle \\ \times \langle L0, SM_S | JM_S\rangle Y_{L'(M_S-M'_S)}(\theta) {\rm e}^{i\sigma_{L'}} \\ \times \frac{S^J_{L'S',LS}(k) - \delta_{L',L}\delta_{S',S}}{ik} {\rm e}^{i\sigma_L}, \end{aligned} \tag{5}$$

where ϵ_{LS} enforces the Pauli principle: $L+S$ has to be even; σ_L is the Coulomb phase shift for the L-wave, and the S-matrix element $S^J_{L'S',LS}$ can be determined from the corresponding "nuclear" partial-wave phase shifts.

The PNC scattering amplitude is calculated by the distorted-wave Born approximation (DWBA)

$$\tilde{f}_{S'M'_S,SM_S}(E,\theta) = -\frac{\mu}{2\pi}\ {}^{(\mp)}\langle \vec{k}', S'M'_S | V_{PNC} | k\hat{z}, SM_S\rangle^{(\pm)}, \tag{6}$$

where $|\vec{k}'| = |\vec{k}|$, $\hat{k}' \cdot \hat{k} = \cos\theta$, and $\mu = m_p/2$ is the reduced mass. Comparing two recent works, Refs. [13] and [5], with the former using DWBA and the latter being numerically exact, treating V_{PNC} as a first-order perturbation is a well-justified approximation.

It should be noted that $A_L^{\rm tot}$, though being well-defined and easily calculable, is not a quantity which an experiment directly measures. There are two major setups for $\vec{p}p$ scattering: the scattering-type (for low-energy protons like Refs. [2,3]) and the transmission-type (for high-energy protons like Ref. [4]) experiments. The former one measures the weighted, average asymmetry within a selected angular range $[\theta_1, \theta_2]$. The latter measures the total asymmetry greater than a critical angle θ_c, as the beam in the angular range of $[0, \theta_c]$ is extracted to analyze the transmission rate so that the total cross section between $[\theta_c, \pi]$ can be inferred. Since none of these experiments has full angular coverage and is able to turn off the Coulomb interaction, some theoretical correction is needed when converting an experimental asymmetry to $A_L^{\rm tot}$. For these issues, we refer readers to Refs. [5,13] and publications of individual experiments for more details.

III. THE VECTOR-MESON EXCHANGE POTENTIAL

The one-meson-exchange PNC NN potential, often used in the literature, refers to the expression given in Ref. [6]. For a pp (nn) system, where only ρ and ω mesons contribute, this potential can be generalized to the following form:

$$\begin{aligned} V_{PNC}^{pp(nn)}(\mathbf{r}) = &-\frac{g_{\rho NN}}{m_N}\left(h_\rho^0 \boldsymbol{\tau}_1\cdot\boldsymbol{\tau}_2 + \frac{h_\rho^1}{2}\left(\tau_1^z+\tau_2^z\right)\right.\\ &\left.+\frac{h_\rho^2}{2\sqrt{6}}\left(3\tau_1^z\tau_2^z - \boldsymbol{\tau}_1\cdot\boldsymbol{\tau}_2\right)\right)\\ &\times\Big((\boldsymbol{\sigma}_1-\boldsymbol{\sigma}_2)\cdot\{\boldsymbol{p}, f_{\rho+}(r)\}\\ &-(\boldsymbol{\sigma}_1\times\boldsymbol{\sigma}_2)\cdot\hat{\boldsymbol{r}} f_{\rho-}(r)\Big)\\ &-\frac{g_{\omega NN}}{m_N}\left(h_\omega^0+\frac{h_\omega^1}{2}\left(\tau_1^z+\tau_2^z\right)\right)\\ &\times\Big((\boldsymbol{\sigma}_1-\boldsymbol{\sigma}_2)\cdot\{\boldsymbol{p}, f_{\omega+}(r)\}\\ &-(\boldsymbol{\sigma}_1\times\boldsymbol{\sigma}_2)\cdot\hat{\boldsymbol{r}} f_{\omega-}(r)\Big), \end{aligned} \tag{7}$$

where m_N represents the nucleon mass, and g_{xNN}'s and h_x^i's denote respectively the strong and the weak meson-nucleon coupling constants for the meson x and isospin i.[1]

The radial functions $f_{x\pm}(r)$ contain important information about the meson-exchange mechanism such as its range and vertex form factor, and will be the main variable to be studied in this work. In the original DDH model, where a point-like ("bare") meson-nucleon vertex is assumed, they are simply related to the Yukawa function $f_x(r)$ as

$$f_{x+}^{\rm bare}(r) = f_x(r) \equiv \frac{e^{-m_x r}}{4\pi r}, \tag{8}$$

$$\hat{\boldsymbol{r}} f_{x-}^{\rm bare}(r) = -i(1+\kappa_x)[\boldsymbol{p}, f_x(r)], \tag{9}$$

where κ_x is the strong tensor meson-nucleon coupling with $\kappa_{\rho,\omega} = \kappa_{V,S}$ (V for isovector and S for isoscalar) respectively. Modifications of the above standard PNC potential to be considered in this work include: (1) variations of the tensor coupling κ_V and the introduction of cutoff form factors at the meson-nucleon vertices, (2) the description of the ρ-meson as a two-pion resonance, and (3) specific PNC meson-nucleon vertices. All these changes involve different forms of $f_{x\pm}(r)$ which will be precised in the following subsections. We also note that $f_{x\pm}(r)$ can have isospin dependence—though it is not manifest in Eq. (7)—and a superscript denoting the isospin will be added whenever more clarification is necessary.

When $f_{x\pm}(r)$ does not have isospin dependence, the isospin matrix elements can be easily evaluated and this gives rise to a V_{PNC}^{pp} depending on two combinations of the weak-coupling constants

$$h_\rho^{pp} = h_\rho^0 + h_\rho^1 + h_\rho^2/\sqrt{6}, \tag{10}$$

$$h_\omega^{pp} = h_\omega^0 + h_\omega^1, \tag{11}$$

and their numbers to be used in our analysis are given in Table I. The set denoted by DDH corresponds to the DDH "best-guess" values [6]. As is known, it roughly accounts for the PNC asymmetries measured at low energy (13.6 and 45 MeV). It could miss however the high-energy asymmetry at 221 MeV as reminded in the introduction (see detailed results in Sec. IV A and Table IV). The other set, "adj.", was fitted by Carlson *et al.* [5] to the experimental values of A_L at the three above energies. Since then, it has been used to make predictions for PNC effects in the np system [20], showing in some cases significant differences from the DDH "best-guess" predictions, especially for the PNC mixing parameter relative to the $^1S_0 - {}^3P_0$ transition, ϵ^0.

TABLE I. Weak coupling constants in units of 10^{-7}.

	h_ρ^{pp}	h_ω^{pp}
DDH [6]	−15.5	−3.04
adj. [5]	−22.3	+5.17

A. Strong coupling constants and monopole form factors

In the analysis by Carlson *et al.* [5], while various modern strong potentials were used to examine the model dependence, the strong coupling constants, $g_{\rho NN}$, $g_{\omega NN}$, κ_V, and κ_S, and the meson-exchange dynamics were fixed to the CD-Bonn model [21]. The introduction of monopole form factors at both the strong and weak meson-nucleon vertices—to be consistent with the Bonn model—results in a modified radial function

[1] We notice that the strong and weak couplings are phase dependent. The convention retained here, usually employed in the field, corresponds to positive values of the former ones when the $f_{x\pm}(r)$ functions are given by the Yukawa-like functions given in Eqs. (8) and (9).

TABLE II. Sets of the strong coupling constants. The cutoffs Λ_ρ and Λ_ω are in units of GeV.

	$g_{\rho NN}$	$g_{\omega NN}$	κ_V	κ_S	Λ_ρ	Λ_ω
S1	2.79	8.37	3.70	−0.12	–	–
S2	2.79	8.37	6.10	0	–	–
S3	2.79	8.37	3.70	−0.12	1.31	1.50
S4	3.25	15.58	6.10	0	1.31	1.50

in V_{PNC}^{pp}:

$$f_{x+}^{\text{mono}}(r) = \frac{e^{-m_x r}}{4\pi r} - \frac{e^{-\Lambda_x r}}{4\pi r}\left[1 + \frac{1}{2}\Lambda_x r\left(1 - \frac{m_x^2}{\Lambda_x^2}\right)\right], \quad (12)$$

$$\hat{\boldsymbol{r}} f_{x-}^{\text{mono}}(r) = -i(1+\kappa_x)\big[\boldsymbol{p}, f_{x+}^{\text{mono}}(r)\big], \quad (13)$$

where Λ_x is the momentum cutoff for x-meson exchange. The values of these parameters are given in the row S4 of Table II. We note that, as suggested by Miller [22], this parameter set, particularly with a large isovector tensor coupling, κ_V, enhances the anapole moment of ^{133}Cs, requiring a value of the πNN coupling, h_π^1, more consistent with expectations or with the absence of effect in ^{18}F [23].

In order to explore the role of the strong coupling constants and the cutoff values, we consider three additional sets, denoted by S1, S2, and S3 in Table II. The set S1 corresponds to strong coupling constants we have been using in our previous works on PNC problems [24,25]. It involves values of $\kappa_V = 3.7$ and $\kappa_S = -0.12$ that are favored by the vector meson dominance. The set S2 mainly differs from the set S1 by a larger value of $\kappa_V = 6.1$. This value came from an analysis of pion-nucleon scattering by Höhler and Pietarinen [15], and was adopted in the Bonn model. The set S3 corresponds to a modified set S1 by introducing the same monopole form factor as Ref. [5]. The consideration of sets S1, S2, and S3 is useful in that the comparison between S1 and S2 gives the dependence on the tensor coupling constants, and the comparison between S1 and S3 shows the role of the hadronic form factors.

Among the different sets considered here, it is not clear at first sight which one is the most realistic [22], and comments with this respect should be done. In absence of information, it seems reasonable to rely on the parameters fixed by some NN interaction model. However, they might possibly account for physics different from that one they are supposed to describe. It has been shown that the large $g_{\omega NN}$ in potential models, like the one in line S4 of Table II, could actually simulate a coherent contribution of bare-ω exchange (with a coupling of the size given in the other lines) and $\rho\pi$ exchange [26]. On the other hand, accounting for hadronic form factors sounds also reasonable at first, but a dispersion approach to the derivation of the NN interaction ignores them by definition. Since form factors imply that the particles have inner structure, their excitations should be considered for consistency. As a matter of fact, there are cases that can be worked out where both effects cancel. This indicates that caution is required in dealing with form factors. Finally, the term involving the tensor coupling is expected to be associated with a hadronic form factor that drops faster than for the other terms, which is most often ignored.

In the following subsection, we present an improved description of the ρ-exchange contribution. It, in particular, involves the physics underlying the increase of κ_V from 3.7 to 6.1, while providing hadronic form factors (including the faster drop-off of the form factor associated with κ_V).

B. Two-pion exchange contribution

In order to account for the two-pion resonance nature of the ρ meson, we follow the work presented in Ref. [16] based on dispersion relations. In this formalism, only stable particles are involved and the ρ meson appears indirectly in the transition amplitude, $N\bar{N} \to \pi\pi$, through its propagator. To satisfy unitarity, the width of the ρ meson has to be accounted for, and this leads to the modification of the free-particle propagator

$$\frac{1}{m_\rho^2 - t'} \to \frac{1}{m_\rho^2 - t' + i\gamma q^3(t')}, \quad (14)$$

where γ is related to the ρ-meson decay width Γ_ρ by

$$\Gamma_\rho = \gamma q^3\left(m_\rho^2\right)/m_\rho, \quad (15)$$

$q(t')$ is defined as

$$q(t') = \sqrt{\frac{t'}{4} - m_\pi^2}, \quad (16)$$

and t' represents the invariant squared mass of the two-pion system in the t-channel of the NN amplitude, on which the integral in the dispersion relation is performed. The above amplitude has to be completed for its PC part by a background contribution involving the exchange in the t-channel of the nucleon and the Δ or N^* resonances (collectively denoted as N^* in the following, in absence of ambiguity). The corresponding PNC part is ignored as it involves new but essentially unknown parameters.

The next step is to introduce the above $N\bar{N} \to \pi\pi$ transition amplitudes in the dispersion relation which allows one to calculate the NN scattering amplitude. In terms of diagrams, the zero-width ρ-meson contribution to the NN interaction, shown in Fig. 1(a), is thus replaced by the sum of contributions depicted in Fig. 1(b) and 1(c). For the intermediate baryon states appearing in the last contribution, we retain, beside the nucleon, the three lowest-lying resonances, $\Delta(1232)$, $N(1440)$ and $N(1520)$ [16].

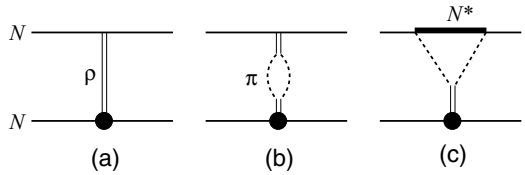

FIG. 1. Graphical representation of ρ exchange as a stable particle (a) or taking into account its possible decay into two pions, (b) and (c). The single solid line denotes a nucleon, the double line a ρ meson, the dashed line a pion and the thick solid line a nucleon or a baryon resonance. These last contributions, which involve intermediate baryons N, Δ and N^*, are collectively denoted here by N^*. The filled circle represents PNC ρNN vertices.

To obtain the potential in configuration space, a standard Fourier transformation has to be performed. The radial functions $f_{\rho+}(r)$ and $f_{\rho-}(r)$ in Eq. (7) for the isoscalar, isovector and isotensor parts now become[2]

$$f_{\rho+}^{2\pi(0,1,2)}(r) = \frac{1}{3(2\pi)^3}\int_{4m_\pi^2}^{\infty} dt' \frac{e^{-r\sqrt{t'}}}{r}\frac{q^3(t')}{\sqrt{t'}} g_{\rho+}(t'), \quad (17)$$

$$f_{\rho-}^{2\pi(0,1,2)}(r) = \frac{1}{3(2\pi)^3}\int_{4m_\pi^2}^{\infty} dt' \frac{e^{-r\sqrt{t'}}}{r} \times \left(1+\frac{1}{r\sqrt{t'}}\right) q^3(t') g_{\rho-}(t'). \quad (18)$$

The spectral functions $g_{\rho+}(t')$ and $g_{\rho-}(t')$ are defined as

$$g_{\rho+}(t') = \frac{f_\rho^2}{\left(m_\rho^2 - t'\right)^2 + \gamma^2 q^6(t')} + \mathrm{Re}\frac{\beta(t') + m_N\alpha(t')}{m_\rho^2 - t' + i\gamma q^3(t')}, \quad (19)$$

$$g_{\rho-}(t') = \frac{f_\rho^2(1+\kappa_V)}{\left(m_\rho^2 - t'\right)^2 + \gamma^2 q^6(t')} + \mathrm{Re}\frac{\beta(t')}{m_\rho^2 - t' + i\gamma q^3(t')}, \quad (20)$$

where

$$\gamma = \frac{f_\rho^2}{6\pi m_\rho}. \quad (21)$$

The quantities, $\alpha(t')$ and $\beta(t')$, appearing in the above equations are given by

$$\alpha(t') = \frac{3}{q(t')\chi^2(t')}\sum_{N^*}\left[\frac{G_{N^*}^A}{q(t')}\left(1 - h\tan^{-1}\frac{1}{h}\right) + \frac{m_N}{2\chi(t')}G_{N^*}^B\left(3h - (1+3h^2)\tan^{-1}\frac{1}{h}\right)\right], \quad (22)$$

$$\beta(t') = -\frac{3}{2q(t')\chi(t')}\sum_{N^*}G_{N^*}^B\left[h - (1+h^2)\tan^{-1}\frac{1}{h}\right], \quad (23)$$

with

$$\chi(t') = \sqrt{m_N^2 - \frac{t'}{4}}, \quad (24)$$

$$h = h(t') = \frac{q^2(t') - \chi^2(t') + m^{*2}}{2q(t')\chi(t')}. \quad (25)$$

The values of the coefficients $G_{N^*}^{A,B}$ used in the present work are given in Table III.

Different values of $f_\rho^2/(4\pi)$ are referred to in the literature. They can be related, for instance, to the decay width of $\rho \to e^-e^+$ or to $g_{\rho NN}$ by the hypothesis of vector meson dominance. In the present estimate, we use the latter. For consistency with $g_{\rho NN} = 2.79$ in the sets S1–S3 (see Table II), $f_\rho^2/(4\pi) = 2.5$ (2.08 was used in Ref. [16]).

TABLE III. Coefficients $G_{N^*}^A$ and $G_{N^*}^B$ appearing in Eqs. (22) and (23): values for the intermediate baryons (nucleon and resonances) retained here.

N^*	$G_{N^*}^A/(4\pi m_\pi)$	$G_{N^*}^B/(4\pi)$
N	0	14.48
$\Delta(1232)$	$-21.8 - 0.97\frac{t'}{m_\pi^2}$	$7.4 - 0.062\frac{t'}{m_\pi^2}$
$N(1440)$	-7.11	2.15
$N(1520)$	$-5.75 - 0.252\frac{t'}{m_\pi^2}$	$1.26 + 0.06\frac{t'}{m_\pi^2}$

If one neglects the contribution from intermediate baryons and takes the limit of $\gamma \to 0$ ($\Gamma_\rho = 0$) in Eqs. (19) and (20), the radial functions $f_{\rho\pm}^{2\pi(0,1,2)}(r)$ simply reduce to the original Yukawa-like ones $f_{\rho\pm}^{\mathrm{bare}}(r)$.

The two-pion exchange interaction also contains a part with an isovector character which results from a non-zero πNN coupling. Its contribution to the PNC asymmetry of interest in this work has been calculated in the past [19]. It has not been considered here however. While it could represent one half of the low-energy measurements with the "best-guess" value of this coupling, there are many reasons to believe that this coupling is actually smaller [7]. The corresponding contribution is therefore expected to play a minor role. On the other hand, this contribution looks like a ρ-exchange one [16] and qualitative results obtained here for the other two-pion exchange contribution, $f_{\rho\pm}^{2\pi(0,1,2)}(r)$, would largely apply to it in any case.

C. Parity-nonconserving ρNN vertex form factor

Meson-nucleon vertex functions are generally written as the product of the coupling constant, defined for an on-mass-shell meson ($q^2 = m^2$), and a form factor which depicts the q^2 dependence. Among various empirical choices, the monopole one is often adopted for the strong vertex, which leads to, e.g., the Bonn potentials [21,27]. As already mentioned in the Sec. III A, the works of Refs. [5,13] involve applying the same monopole form factor also to the weak vertex, which gives rise to modified radial functions as in Eqs. (12) and (13). However, one can certainly speculate about other possibilities.

In the DDH work [7], the coupling constant receives three contributions: "factorization," "parity admixture" and "sea quarks." For simplicity, they have been taken as constant. The two last contributions were estimated by relying on the $SU(6)_W$ symmetry and experimental information from non-leptonic hyperon decays but the authors also worried about symmetry-breaking effects. These ones could be sizable for the "parity-admixture" contribution to the isoscalar ρNN coupling, which can be shown to vanish at $q^2 = 0$.[3] This result is due to the cancellation of two contributions with the same topology but involving intermediate quarks with negative

[2]The isovector PNC ρNN coupling was not part of theoretical frameworks by the time the above work [16] was written. There is no more reason to ignore it now although the corresponding contribution is expected to be quite small.

[3]This contribution is absent for the isotensor ρNN coupling and both isoscalar and isovector ωNN couplings. The vanishing of the contribution at $q^2 = 0$ for the isoscalar ρNN coupling has some relationship with an anapole moment contribution.

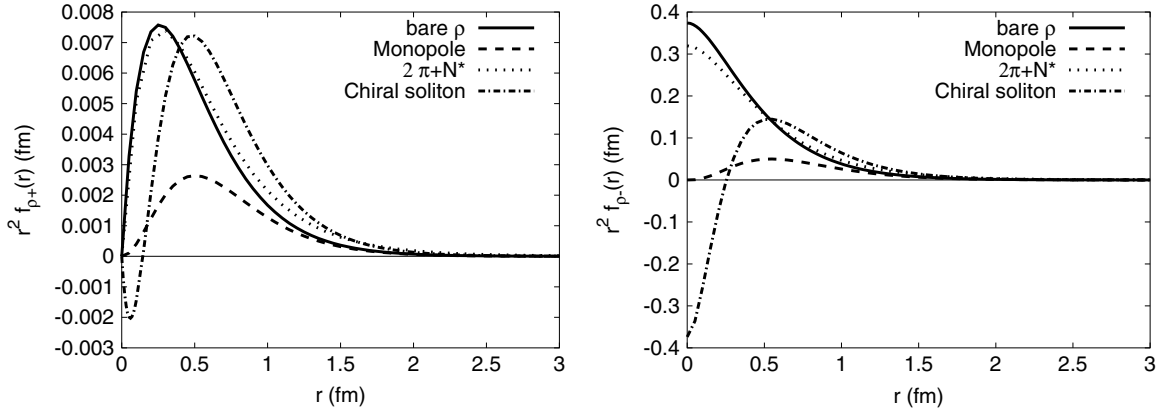

FIG. 2. Yukawa function (bare-ρ, continuous) and modified ones due to form factors with a monopole type at both PC and PNC vertices (Monopole, dashed), to 2π and N^* corrections ("$2\pi + N^*$", dot), and to PNC form factors obtained from the chiral-soliton model calculation [11] (Chiral soliton, dot-dashed). The left panel is for $f_{\rho+}(r)$, and the right one for $f_{\rho-}(r)$. Expressions of the potentials are given in the text, Eqs. (8), (9), (12), (13), (19), (20), (27), (28), and parameters entering the monopole and chiral-soliton ones, Λ and Λ', are given the unique value 1.31 GeV.

and positive energies. While the first one is included by using the $SU(6)_W$ symmetry and could be appropriate for an on-mass-shell meson, the effect of the second one is ignored. To account for the expected cancellation, the "parity-admixture" contribution to the isoscalar ρNN coupling was suppressed by a factor 4 in getting the "best-guess" values. A refined estimate would suppose to calculate the q^2 dependence of the coupling constant, which was done by Kaiser and Meissner in their framework [11]. Although there exists no detailed comparison, their results tend to support the above analysis. The q^2 dependence is especially important for the isoscalar ρNN coupling. It evidences a feature which is somewhat unusual for current form factors but is a signature of the underlying dynamics: a change of sign occurs at $q^2 = q_0^2 - \boldsymbol{q}^2 \simeq -m_\rho^2$.

We now consider the effect of inserting the above momentum dependence in the PNC NN interaction. Consistently with the non-relativistic approach used here, we neglect the energy transfer carried by the meson and therefore assume $q^2 \simeq -\boldsymbol{q}^2$ in the following. The isoscalar PNC ρNN vertex form factor, $\tilde{F}_\rho^{\mathrm{KM}(0)}(\boldsymbol{q}^2)$, in Ref. [11] can thus be approximately parametrized as

$$\tilde{F}_\rho^{\mathrm{KM}(0)}(\boldsymbol{q}^2) = \left(1 - 2\frac{\boldsymbol{q}^2}{\boldsymbol{q}^2 + \Lambda'^2}\right). \tag{26}$$

At low-momentum transfer, the parameter Λ' has the same effect as usual cutoff parameters but its role differs at high momentum transfer (hence a different notation). The sensitivity to this parameter will be studied in the later section. Assuming the corresponding strong vertex is still a point-like one, the radial functions for the isoscalar ρ exchange, modified by Eq. (26), now reads

$$f_{\rho+}^{\mathrm{KM}(0)}(r) = \frac{\Lambda'^2 + m_\rho^2}{\Lambda'^2 - m_\rho^2} f_\rho(r) - \frac{2\Lambda'^2}{\Lambda'^2 - m_\rho^2} f_{\Lambda'}(r), \tag{27}$$

$$f_{\rho-}^{\mathrm{KM}(0)}(r) = -i(1+\kappa_\rho)[\boldsymbol{p}, f_{\rho+}^{\mathrm{KM}(0)}(r)]. \tag{28}$$

In the limit $\Lambda' \to \infty$, $f_{\rho+}^{\mathrm{KM}(0)}(r)$ recovers the standard Yukawa function $f_\rho(r)$. In a special case where $\Lambda' = m_\rho$, corresponding to the above mentioned change of sign at $q^2 \simeq -m_\rho^2$, $f_{\rho+}^{\mathrm{KM}(0)}(r)$ remains finite

$$f_{\rho+}^{\mathrm{KM}(0)}(r) = \frac{1}{4\pi r} \mathrm{e}^{-m_\rho r}(m_\rho r - 1), \tag{29}$$

despite the presence of the factor $\Lambda'^2 - m_\rho^2$ in the denominator.

D. Resulting potentials

The masses of π, ρ and ω mesons are set to be 139.0, 771.0 and 783.0 MeV respectively, throughout the calculations. Plotted in Fig. 2 are $f_{\rho+}(r)$ and $f_{\rho-}(r)$ multiplied by r^2 which appears in the r-space integration. The potentials with bare-ρ exchange, the monopole form factor, the $2\pi + N^*$ corrections and the PNC chiral-soliton form factor are represented respectively by solid, dashed, dotted and dot-dashed lines.

Compared to the bare-ρ-exchange potential, the $2\pi + N^*$ corrected ("$2\pi + N^*$") one gives a non-negligible enhancement in the range $0.5 \leqslant r \leqslant 2$ fm. In the remaining regions, however, these two potentials are almost indistinguishable. For the potentials with form factors, we show results with $\Lambda' = 1.31$ GeV and $\Lambda_\rho = 1.31$ GeV for the chiral-soliton and monopole ones, respectively. Both of them give significant difference from bare-ρ and "$2\pi + N^*$" potentials at $r \leqslant 2$ fm. The chiral-soliton form factor enhances the potential substantially at $0.4 \leqslant r \leqslant 2$ fm, drops rapidly at around $r \approx 0.4$ fm and changes sign at $r \leqslant 0.2$ fm. The change of sign can give a negative contribution to the matrix elements, but the quantitative estimation is dependent on the shape of the wave functions. With different Λ' values, the shape of the potential changes. For a value smaller than 1.31 GeV, the change of sign is shifted to larger r values, and the enhancement in the intermediate range becomes more significant than for the present potential. On the other hand, if one increases the Λ' value, the potential becomes more similar to the bare-ρ one. We will show this behavior explicitly when we discuss the results. Contrary to the PNC chiral-soliton form factor,

TABLE IV. Sensitivity of the PNC asymmetry, $A_L(\times 10^7)$, to different choices of weak and strong coupling constants, or to monopole form factors (see Tables I and II for their values) and comparison with experiment.

Weak / Strong	DDH				Adj.	Exp.[a]
	S1	S2	S3	S4	S4	
13.6	−0.96	−1.33	−0.66	−1.13	−0.92	-0.95 ± 0.15 [2]
45	−1.73	−2.39	−1.16	−2.00	−1.59	-1.50 ± 0.23 [3]
221	0.43	0.75	0.25	0.52	0.85	0.84 ± 0.29 [4]

[a]These values are taken from Ref. [5], assuming the theoretical corrections have been made.

a monopole form factor gives suppression in magnitude over the whole r region. This suppression will give matrix elements smaller than in the remaining three cases. More importantly, a monopole form factor makes the potential more sensitive to the cutoff value than the PNC chiral-soliton form factor is to the value of Λ'. We will argue about this point in the forthcoming results.

Concluding this section, an important observation should be made with respect to the motivation of the present work. In comparison to the standard ρ-exchange potential, some of the variations we consider tend to make its range longer. At first sight, the feature which can possibly enhance the contribution of P to D NN states with respect to the S to P ones is desirable. This can be checked by calculating the plane-wave Born amplitude, but a definitive answer requires a full calculation with distorted wave functions.

IV. NUMERICAL RESULTS AND DISCUSSION

We here discuss qualitatively the effects of the different variations on the meson-exchange potential laid down in the previous section.

A. Effect of the coupling constants and monopole form factors

In Table IV, the results with various chosen parameter sets (see Tables I and II for their values) are presented. The effect of the coupling constants is straightforward: larger coupling constants give larger asymmetries. As shown in Ref. [1] that the $S-P$ transition dominates at the low energies, while the $P-D$ transition does at the high energies, the $S-P$ transition amplitude is approximately proportional to

$$h_\rho^{pp} g_{\rho NN}(\kappa_V + 2) + h_\omega^{pp} g_{\omega NN}(\kappa_S + 2), \tag{30}$$

and the $P-D$ transition amplitude to

$$h_\rho^{pp} g_{\rho NN}\kappa_V + h_\omega^{pp} g_{\omega NN}\kappa_S. \tag{31}$$

Beginning the discussion with a comparison of the predictions and measurements, we observe that the S1-set results agree with the low-energy measurements. At 221 MeV, the result is smaller than the lowest experimental value by about 22%. For the set S2, the situation is opposite: the result at 221 MeV is within the error bar, but those at low energies are off. Since the asymmetry can be well approximated by Eqs. (30) and (31), which are linearly dependent on the strong coupling constants g_{xNN} and κ's, we conclude that those good at low energy are not good at 221 MeV, and vice versa. As expected, the asymmetry is sensitive to the strong coupling constants, but this is almost irrelevant to the resolution of the problem raised in the introduction.

We now consider in more detail the sensitivity to the isovector tensor coupling κ_V. This can be done by comparing results of sets S2 and S1, or S4 and S3. Evaluating Eq. (30) with S2 and S1, we obtain the ratio S2/S1 $(S-P) \simeq 1.36$. This value is comparable to the ratios of S2/S1 at 13.6 and 45 MeV, 1.39 and 1.38, respectively. Equation (31) gives S2/S1 $(P-D) \simeq 1.68$, and this value is close to S2/S1 at 221 MeV, 1.74. In a similar way, we can compare S4 and S3. We have the ratios S4/S3 $(S-P) \simeq 1.71$ and S4/S3 $(P-D) \simeq 1.96$. Our calculation gives 1.71 and 1.72 at 13.6 and 45 MeV, respectively, and 2.10 at 221 MeV. In both cases, it is found that changing κ_V from 3.7 to 6.1 enhances the prediction for the high-energy point with respect to the low-energy ones. The effect, which is of the order of 25%, goes in the direction we looked for. However, for the set S1, enhancement due to a larger value of κ_V is still lacking to fit the high-energy asymmetry within the experimental error bar.

The role of monopole form factors can be understood by comparing results of sets S3 and S1 (or S4 and S2 after correcting for different strong couplings in this case). The ratios are 0.69, 0.69, and 0.58 at 13.6, 45, and 221 MeV, respectively (or 0.73, 0.72, and 0.59). One sees a clear indication that the effect of monopole form factors is in favor of S to P transitions, contrary to what we would naively expect from a longer-range interaction. This point will be further examined later on after other similar long-range effects are also considered.

For a part, the above results can be understood from the behavior of the potentials. In Fig. 3, the left panel shows the Yukawa potential modified by monopole form factors, with a multiplication factor r^2. The smaller the cutoff value is, the smaller is the potential for all r. Thus, with a smaller cutoff value, the asymmetry is also smaller in magnitude. The large sensitivity of the potential to the cutoff value as Fig. 3 shows, has its origin in the expression of the squared monopole form factor in momentum space, $[(\Lambda^2-m^2)/(\Lambda^2+\boldsymbol{q}^2)]^2$. This form, which is consistent with the definition of couplings made for on-mass-shell mesons, implies an overall suppression of PNC amplitudes at low energy by a factor $[(\Lambda^2-m^2)/(\Lambda^2)]^2 (= 0.43$ for $\Lambda = 1.31$ GeV). This behavior differs from the one evidenced by other potentials considered below where the factor under discussion is essentially absent. On the other hand,

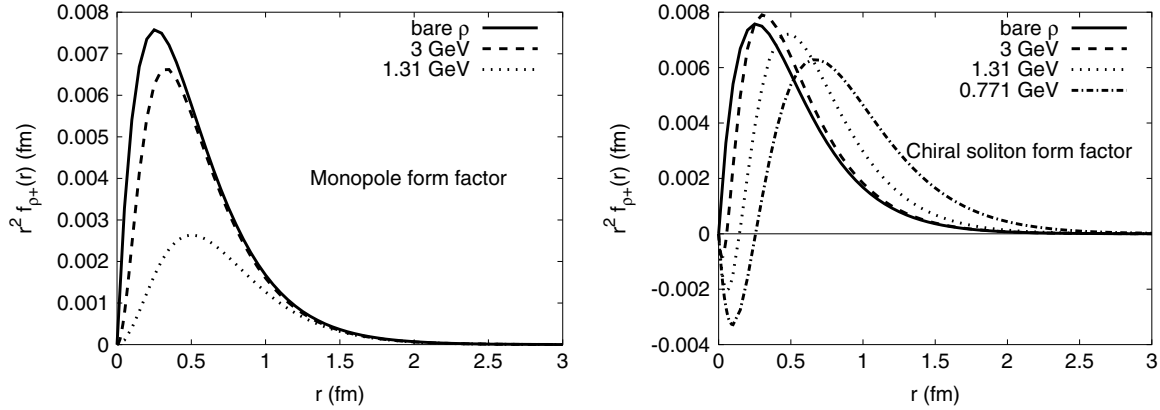

FIG. 3. Modified Yukawa functions multiplied by r^2: with the square of monopole form factor (left panel) and the PNC chiral-soliton form factor (right panel). For illustration, the cutoff Λ is given the values ∞ (bare), 3, and 1.31 GeV in one case while the parameter Λ' assumes the values ∞ (bare), 3, 1.31, and 0.771 GeV in the other case.

the difference between the above suppression factor and the one deduced in the previous paragraph by comparing S3 and S1 results indicates that the effect of the potential occurs at distances larger than what the position of maxima in Fig. 3 suggests.

B. Effect of the 2π and N^* corrections

The effect of the $2\pi + N^*$ corrections is investigated with the strong parameter sets S1 and S2, and the DDH "best-guess" values for the weak coupling constants. The results are summarized in Table V. In the column "$2\pi + N^*$", the numbers in the parentheses represent the ratios of results ("$2\pi + N^*$")/(bareρ).

The "$2\pi + N^*$" result evidences a relatively larger enhancement at 13.6 MeV than at the remaining two energies, but as a whole, the ratios are similar. For the set S1, the "$2\pi + N^*$" potential increases the asymmetry by 0.26, 0.38, and 0.09 at 13.6, 45, and 221 MeV, respectively (in units of 10^{-7}). Consequently the low-energy asymmetries exceed the experimental upper limit while the high-energy one is still below. For the set S2, the amount of increase is larger than for the set S1: 0.35, 0.53, and 0.17 at 13.6, 45, and 221 MeV, respectively (again in units of 10^{-7}). Thus, the low-energy predictions, which are already out of the experimental error bars with the ρ-exchange potential, are further away from experiment. Meanwhile, a relatively small increase of the high-energy asymmetry keeps the prediction within error bars.

To get some insight into the above results, it is interesting to look at the potentials in Fig. 2. At $r \geqslant 2$ fm, they show a similar behavior. In comparison to the bare-ρ potential within the range $0.4 \leqslant r \leqslant 2$ fm, $f^{2\pi}_{\rho+}(r)$ is sizably larger but $f^{2\pi}_{\rho-}(r)$ is slightly smaller. In the range $r \leqslant 0.4$ fm, $f^{2\pi}_{\rho+}(r)$ is very similar but $f^{2\pi}_{\rho-}(r)$ is clearly smaller. From the result of the asymmetry in Table V, one can deduce that the suppression of $f^{2\pi}_{\rho-}(r)$ at short distances does not much affect the magnitude of the asymmetry. Therefore, roughly speaking, a good deal of the difference in the results comes from the difference of the potentials in the region $0.4 < r < 2$ fm and the contribution from $r < 0.4$ fm is negligible.

While the enhancement of the interaction in the range $0.4 < r < 2$ fm can explain enhanced asymmetries, an enhancement of asymmetry at the higher energy point with respect to the low ones, as one would expect from a longer-range interaction, does not show up. Though the effect is small ($0 \sim 3\%$), it is opposite to what could be naively expected. It is interesting to compare the results with those obtained from using the plane-wave Born approximation (PWBA). The enhancement of the asymmetry at low energy would be about 12% while it reaches 26% at high energy (the enhancement for the P to D transition at low energy is about 60%).

TABLE V. Sensitivity of the PNC asymmetry, $A_L(\times 10^7)$, to the effect of the finite ρ-width correction of the weak potential. Weak coupling constants are fixed to the DDH "best-guess" values. Two sets of strong couplings, S1 and S2, are considered. The numbers in the parentheses represent the ratios ("$2\pi + N^*$")/(bare-ρ).

	S1		S2		Exp.
	Bare-ρ	"$2\pi + N^*$"	Bare-ρ	"$2\pi + N^*$"	
13.6	−0.96	−1.22 (1.26)	−1.33	−1.68 (1.25)	-0.95 ± 0.15
45	−1.73	−2.11 (1.21)	−2.39	−2.92 (1.22)	-1.50 ± 0.23
221	0.43	0.52 (1.22)	0.75	0.92 (1.22)	0.84 ± 0.29

As mentioned in Sec. III A, the enhanced κ_V value, 6.1, could account for the physics we included here in allowing for the contribution of nucleon and baryon resonances to the πN scattering amplitude (or the $N\bar{N} \to \pi\pi$ amplitude). Therefore, results denoted "$2\pi + N^*$" with S1 and bare-ρ with S2 in Table V should not be independent. This is supported for a part by the fact that both results deviate from the bare-ρ S1 contribution by relatively the same amount for the low-energy measurements (roughly 24% and 38%). The difference is larger for the high-energy point (22% and 74%), but this could be due to the approximate character of treating the effect of extra contributions to the πN scattering amplitude by a constant number. In principle, the κ_V contribution is expected to be associated with a form factor that decreases faster than for the other contributions.

C. Effect of the PNC vertex form factor

Results with the monopole form factor have been discussed at the beginning of the present section (see Table IV). We here consider the effect of the PNC chiral-soliton form factor for the isoscalar ρNN coupling. As this form factor could involve some uncertainty, we also looked at variations of the cutoff parameter Λ' in Eq. (26). Besides the value $\Lambda' = 0.771$ GeV, which approximately fits Kaiser and Meissner's estimate [11], we consider the values 1.31 and 3 GeV. The first of these last values fits the low-momentum dependence of the monopole form factor used by Carlson *et al*. and the second allows one to make the transition to the standard point-like ρNN coupling. The larger Λ's are probably closer to the one inferred from the DDH work, though quite uncertain. Strong coupling constants are picked up from the set S1, and DDH "best guess" values are used for the weak coupling constants. The results with different strong coupling constants, e.g., S2, can be easily deduced from Eqs. (30) and (31).

Looking at the results given in Table VI, it is seen that the magnitude of the asymmetry increases when the parameter Λ' becomes smaller. This can be understood from the behavior of the potential. In Fig. 3, we plot the modified Yukawa potential multiplied by r^2 for the PNC chiral-soliton form factor (right). With a smaller Λ' value, the position of the peak is shifted to larger r, and the curve becomes broader. This behavior leads to a large enhancement in the range $0.5 \leqslant r \leqslant 2$ fm. In the result with the $2\pi + N^*$ corrections, we discussed that a large portion of the difference in the asymmetry is expected to be originated from the different behavior of the potential in the range $0.4 < r < 2$ fm. The behavior of $f_{\rho+}^{\rm KM}(r)$ and $f_{\rho-}^{\rm KM}(r)$ in Fig. 2 supports this conjecture; and though these functions even change sign at $r \leqslant 0.2$ fm, enhanced results are still found. A smaller Λ' value gives rise to a more enhanced potential in the range $0.4 < r < 2$ fm and consequently, this gives a larger magnitude of asymmetry.

TABLE VI. Sensitivity of the PNC asymmetry, $A_L(\times 10^7)$, to the effect of a specific correction of the isoscalar PNC ρNN vertex. Results are presented for different values of the parameter Λ', introduced in Eqs. (27) and (28). The bare-meson exchange is adopted for the other components of the PNC potential. Set S1 is used for the strong parameters, and DDH "best-guess" values for the weak coupling constants.

Λ' (GeV)	Bare	3	1.31	0.771
13.6	−0.96	−1.04	−1.33	−1.69
45	−1.73	−1.88	−2.38	−2.92
221	0.43	0.47	0.61	0.67

Similarly to the effect discussed in the previous section, the enhancement of the potential in the range $0.5 \leqslant r \leqslant 2$ fm can explain the enhancement of the asymmetries calculated in this section with respect to the bare-ρ ones. Again, the enhancements are larger at low than at high energy (roughly 73% and 56% for $\Lambda' = 0.771$ GeV) but the relative difference is more obvious here (17% instead of $0 \sim 3\%$). It is interesting to compare the above results with the PWBA ones. In this case, the effect of the form factor under consideration provides a slight suppression at low energy while, at high energy, it leads to a large enhancement, 80% for $\Lambda' = 0.771$ GeV (a factor 3 for the P to D states transition at low energy). These results evidence a striking feature. While the enhancement for the P to D states transition amplitude at high energy in PWBA is more or less recovered by the actual DWBA calculation, the appearance of an enhancement for the S to P states transition amplitude at low energy in PWBA is much less expected by DWBA. To some extent, this confirms the conclusion from considering similar longer-range forces as due to monopole form factors or a non-zero width of the ρ meson that: contrary to a naive expectation, a longer-range force does not necessarily imply an enhancement of P to D states transition amplitudes at high energy over the S to P states one at low energy.

Somewhat surprised by this last result, we looked for an explanation. It turns out that both the $^1S_0$ and $^3P_0$ wave functions entering the S to P transition amplitude are strongly suppressed at short distances in the AV18 model, which we used to describe the strong NN interaction. This suppression acts the same way as the centrifugal barrier favors Born amplitudes with higher orbital angular momenta. However, in AV18, the suppression for the $^1S_0$ and $^3P_0$ is even stronger than the one for $^3P_2$ and $^1D_2$, so an opposite situation occurs here: a longer-range PNC force enhances the S to P transition amplitude with respect to the P to D one. This feature is largely due to the $^3P_0$ wave function where the effect of a short-range repulsion extends to medium distances. Were this wave function similar to the $^3P_2$ one, quite different results would have been obtained instead. The effect of a longer-range interaction would then be more similar to what is expected from considering the PWBA alone. In Ref. [5], other strong potential models were also considered and no big model dependence was found. Therefore, it can be expected roughly that the above conclusion applies for cases other than AV18.

D. Fitting the weak coupling constants

Motivated by the values of PNC coupling constants obtained in an earlier analysis [5], we looked in the present work for possible effects that could affect its conclusions. We consider in this subsection the quantitative consequences of these effects on the coupling constants.

We first notice that none of the cases we considered allows one to reproduce the central values of measurements

by relying on presently known predictions of PNC meson-nucleon couplings. While ρ exchange dominates, ω exchange must necessarily have a sign opposite to what is expected, confirming Carlson *et al.*'s analysis, whose main qualitative features were reminded in the introduction. A question which remains of particular interest is whether the size of the ωNN coupling can be made more consistent with expectations. Before entering into details, we mention that our own results for the ρNN and ωNN couplings, $h_\rho^{pp} = -22.2 \times 10^{-7}$ and $h_\omega^{pp} = 5.28 \times 10^{-7}$, slightly differ from Carlson *et al.*'s ones when the same set of strong couplings, S4, is used. The discrepancies can be reasonably understood as due to minor differences in the inputs.

We begin with the S1 set of strong couplings, for which a qualitative understanding of the result has been reminded in the introduction. A least-χ^2 fit gives $h_\omega^{pp} = 10.5 \times 10^{-7}$ and $h_\rho^{pp} = -25.9 \times 10^{-7}$. The difference with Carlson *et al.*'s result for h_ω^{pp} is primarily due to that one in the strong coupling constant $g_{\omega NN}$. The absence of difference for h_ρ^{pp} is somewhat accidental and results from the cancellation of different effects involving the tensor coupling, κ_V, the strong coupling constant, $g_{\rho NN}$, and the monopole form factor, with some being separately discussed below.

Looking now at the results for the set S2, it is found that the ωNN coupling obtained from a least-χ^2 fit, $h_\omega^{pp} = 7.2 \times 10^{-7}$, is smaller than in the previous case as expected from the discussion of results in Sec. IV B, showing the favorable character of an enhanced value of the isovector tensor coupling, κ_V, for the problem under consideration in this work. A value of the ρNN coupling smaller in magnitude is also obtained, $h_\rho^{pp} = -16.3 \times 10^{-7}$. Let us elaborate this point in more detail. Sets S2 and S1 differ by the values of the tensor couplings, κ_S and κ_V. Since $|\kappa_S| << \kappa_V$, Eq. (31) for the $P - D$ transition amplitude approximately implies $h_\rho^{pp} \propto 1/\kappa_V$. One therefore expects that the ratio of the fitted values, $h_\rho^{pp}(S2)/h_\rho^{pp}(S1)$, be close to the ratio of the tensor couplings, $\kappa_V(S1)/\kappa_V(S2)$. The approximate equality of the ratios, 0.63 and 0.61, respectively, confirms that the ω contribution to the corresponding amplitude is small. For the set S1, its contribution to the asymmetry at high energy amounts to 4%. More generally, the fitted value of h_ρ^{pp} depends on the strong coupling constant as $1/(g_{\rho NN}\kappa_V)$. This implies that the contribution of the term $h_\rho^{pp} g_{\rho NN}\kappa_V$ to the $S - P$ transition amplitude, represented by Eq. (30), is approximately the same for the sets S1 and S2. The remaining term, $2h_\rho^{pp} g_{\rho NN} + h_\omega^{pp} g_{\omega NN}(2 + \kappa_S)$, should be therefore the same too. The value of h_ω^{pp} can be fitted so that this term is the same, regardless of the strong coupling constant. Considering the case discussed above where κ_V increases, leading to an increase of h_ρ^{pp} (algebraically), it appears that the first contribution to the remaining term, $2h_\rho^{pp} g_{\rho NN}$, increases with the consequence that the other term $h_\omega^{pp} g_{\omega NN}(2 + \kappa_S)$ has to decrease. This implies that h_ω^{pp} decreases. The value so obtained is close to the fit one. As will be shown for the results for the set S3, h_ω^{pp} is also sensitive to the value of the strong coupling, $g_{\omega NN}$.

As argued at the end of Sec. III A, a partly improved version of the above results obtained with the set S2 could be given by the "$2\pi + N^*$" ones with the set S1. It is therefore expected that the corresponding fitted couplings should tend to evidence the same departures to the S1-set results. The value obtained in the present case for the ρNN coupling, $h_\rho^{pp} = -21.1 \times 10^{-7}$, is half way between the results for the S1 and S2 sets. The expectation is verified for a part, suggesting that the physics which has led to introduce an enhanced value of κ_V is not fully accounted for. The effect of an approximate treatment of the underlying physics could have more important consequences for the ωNN coupling. This one, given by $h_\omega^{pp} = 11.7 \times 10^{-7}$, remains close to the S1-set result. This feature indirectly indicates that the 2π correction scales the ρ-exchange contribution to the low- and high-energy asymmetries by the same factor, allowing one to account for its effect by modifying the ρNN coupling. The result is that the ωNN coupling is essentially unchanged in the fit procedure. The lower value of the ωNN coupling obtained with the S2 set could therefore be questionable to some extent.

Pursuing the discussion with the results for the set S3, which was intended to look at the effect of monopole form factors often introduced to describe hadronic vertices, it is found that the fitted values of the couplings, $h_\omega^{pp} = 14.6 \times 10^{-7}$ and $h_\rho^{pp} = -41.1 \times 10^{-7}$, are significantly increased (in size) with respect to the previous ones. The difference with Carlson *et al.*'s results comes mainly from different values of the strong couplings and of κ_V. The most important one for the main purpose of the present paper is due to the value of $g_{\omega NN}$, almost a factor 2, which explains a large part of the discrepancy between the fitted values of h_ω^{pp}. There are other significant differences but, due to cancellations, they have not much effect on the PNC ωNN coupling. Taking into account that the product $g_{\rho NN} h_\rho^{pp} \kappa_V$ is mainly determined by the high-energy point, the difference in the value of κ_V is largely compensated by a change in h_ρ^{pp}. Differences between the sets S3 and S4 for other ingredients ($g_{\rho NN}$ and κ_s) have a minor effect. Thus, the comparison of results for these two sets of strong couplings shows that smaller (and more reasonable) values could be obtained for the weak couplings by increasing the size of the strong ones but, while this could be suggested by the phenomenology of the strong *NN* interaction, there is no theoretical justification.

Finally, as for the effects of the weak vertex form factors, the result for the ωNN coupling reflects the discussion of the asymmetries in Sec. IV C. The fitted value tends to increase when Λ' decreases. It is given by $h_\omega^{pp} = 11.5 \times 10^{-7}$ and 15.2×10^{-7} at $\Lambda' = 1.31$ and 0.771 GeV respectively (correspondingly, $h_\rho^{pp} = -16.8 \times 10^{-7}$ and $h_\rho^{pp} = -14.1 \times 10^{-7}$). Strictly speaking, the last values obtained for h_ρ^{pp} only apply to h_ρ^0 as only the isoscalar PNC form factor is taken into account (the isovector and isotensor vertices are still taken as point like). However, to a good approximation, it can be considered that the fit determines an effective h_ρ^{pp} coupling given by $h_\rho^0 + 0.7(h_\rho^1 + h_\rho^2/\sqrt{6})$ for $\Lambda' = 1.31$ GeV and $h_\rho^0 + 0.5(h_\rho^1 + h_\rho^2/\sqrt{6})$ for $\Lambda' = 0.771$ GeV. From what is left out, which is not expected to be large, it is in principle possible to get an extra constraint on the isovector and isotensor couplings. The statistical significance of the result is expected to be smaller than the h_ω^{pp} one, however.

V. CONCLUSION

We considered the PNC asymmetry in $\vec{p}p$ scattering at the energies 13.6, 45 and 221 MeV, where experimental data are available. In a recent analysis [5], ρNN and ωNN weak coupling constants were fitted to reproduce the experimental data. Though the resulting values are within the reasonable range given in Ref. [6], the fitted ωNN coupling constant is opposite in sign to most of the theoretical estimates. Employing AV18 as a strong interaction model, we investigated the role of the effects such as different strong coupling constants, cutoffs in the regularization of the PNC meson-exchange potential, long-range contributions to its ρ-exchange component and PNC form factors of the isoscalar ρNN vertex.

As expected, the asymmetry is sensitive to the strong coupling constants, on which it depends linearly. Assuming the DDH "best-guess" values for the weak couplings, it was found that all three experimental data cannot be satisfied simultaneously with any of the strong coupling sets considered in this work. In one case, low-energy results are within the experimental errors but the high-energy one is not, and vice versa in the other. Comparison of the results with and without monopole form factors shows a significant effect. For the cutoff value $\Lambda = 1.31$ GeV, asymmetries are suppressed by about $30 \sim 40\%$. This strong dependence on the cutoff value qualitatively agrees with the one shown in a different way in Ref. [5]. Fitting the weak couplings to the measurements, the authors found that a decrease of the cutoff value by a factor 0.8 enhances the fitted values of h_ρ^{pp} and h_ω^{pp} from -22.3×10^{-7} and 5.17×10^{-7} to -106.7×10^{-7} and $+14.63 \times 10^{-7}$, respectively [5]. The 2π-exchange contribution to the bare-ρ-exchange potential gives a sizable enhancement at both low and high energies. The ratio of enhancement is, however, similar but slightly larger at 13.6 MeV than that at 45 and 221 MeV. Consequently, with the 2π exchange in the PNC potential, the asymmetries at low energies exceed the experimental ranges, and that at 221 MeV is close to or within the error bar. Simply speaking, the 2π contribution does not change the high vs. low energy trend found in the case of using the bare-meson-exchange potential. The results with a specific PNC form factor show its strong influence too. The larger is the change in the potential, the larger is the magnitude of the asymmetry regardless of the energy: similar to the case including 2π exchange. Concluding this part of our work based on the DDH "best-guess" values for the weak couplings, we did not find any effect that could allow one to simultaneously describe the measurements of the asymmetries at low and high energies.

As is well known, predictions for the weak ρNN and ωNN couplings are uncertain and can largely vary in some range. One can thus look for values of these couplings which could fit the above measurements. The striking feature is that in all cases we considered the h_ω^{pp} coupling constant has a positive sign, opposite to the DDH "best-guess" one. This is not therefore a surprise if the above studies with the DDH "best-guess" values could not provide a good description of the measurements. The sign agrees with Carlson *et al.*'s one [5] but the size, which assumes some improvements in this work, is generally larger, making it more difficult for the h_ω^{pp} coupling so obtained to be accommodated in the expected range. Thus, the discrepancy that motivated the present work, far to be reduced, is enhanced.

Interestingly, the possibility that the ωNN coupling be positive was considered in the past to explain the ratio of the proton-nucleus force, determined from PNC effects in some complex nuclei, to the proton-proton one, determined from PNC effects in $\vec{p}p$ scattering at low energy [7]. It was however discarded due to a low statistical significance and the absence of theoretical support. With results from incorporating the high-energy point in the analysis of $\vec{p}p$ scattering (Ref. [5] and present work), the above prospect becomes less unlikely.

We here consider three issues. The first one is that the value of the fitted ωNN coupling, its sign in particular, is correct. This implies that present hadronic estimates are missing important contributions. With this respect, one should distinguish bare and dressed couplings that could include rescattering effects (loop corrections) [28]. Including some phenomenology however, it is not clear how much present estimates should be corrected for them. The second issue is the possible existence of large corrections to the PNC single-meson exchange potential [29]. This concern has motivated various approaches dealing more directly with *NN* scattering amplitudes, in the past [30,31] and quite recently [32]. Multimeson exchanges or retardation effects are known to provide large corrections in the strong-interaction case and there is no reason it should be different here. Along the same lines, one could also cite relativistic corrections which, for vector-meson exchanges, could be important [14]. The last issue concerns the experiment, especially at the highest energy of 221 MeV. The discussion throughout the paper is based on the absence of error bar. Assuming minor adjustments of the meson-nucleon couplings to the low-energy points, current predictions for the highest-energy point may be off by a factor two for the central value, but only by one and a half standard deviation when the experimental error is accounted for. On the other hand, the PNC experiments are difficult ones and a naive interpretation of the error bar does not necessarily give a good indication of where a more accurate measurement would sit. A tendency to overestimate the real asymmetries has often been observed. Whatever the issue, we believe all of them quite exciting because further studies will be required to determine the right answer.

ACKNOWLEDGMENTS

We are grateful to B. F. Gibson for valuable comments. The work of CPL was supported by the Dutch Stichting vor Fundamenteel Onderzoek der Materie (FOM) under program 48 (TRIμP). This work was supported by the Korea Research Foundation Grant funded by Korea Government (MOEHRD, Basic Research Promotion Fund) (KRF-2005-206-C00007).

[1] M. Simonius, Can. J. Phys. **66**, 548 (1988).
[2] P. D. Eversheim *et al.*, Phys. Lett. **B256**, 11 (1991).
[3] S. Kistryn *et al.*, Phys. Rev. Lett. **58**, 1616 (1987).
[4] A. R. Berdoz *et al.*, Phys. Rev. Lett. **87**, 272301 (2001).

[5] J. Carlson, R. Schiavilla, V. R. Brown, and B. F. Gibson, Phys. Rev. C **65**, 035502 (2002).
[6] B. Desplanques, J. F. Donoghue, and B. R. Holstein, Ann. Phys. (NY) **124**, 449 (1980).
[7] B. Desplanques, Phys. Rep. **297**, 1 (1998).
[8] B. Desplanques, Nucl. Phys. **A335**, 147 (1980).
[9] G. B. Feldman, G. A. Crawford, J. Dubach, and B. R. Holstein, Phys. Rev. C **43**, 863 (1991).
[10] N. Kaiser and U. G. Meissner, Nucl. Phys. **A489**, 671 (1988); **A499**, 699 (1989).
[11] N. Kaiser and U. G. Meissner, Nucl. Phys. **A510**, 759 (1990).
[12] F. Nessi-Tedaldi and M. Simonius, Phys. Lett. **B215**, 159 (1988).
[13] D. E. Driscoll and G. A. Miller, Phys. Rev. C **39**, 1951 (1989).
[14] D. E. Driscoll and G. A. Miller, Phys. Rev. C **40**, 2159 (1989).
[15] G. Höhler and E. Pietarinen, Nucl. Phys. **B95**, 210 (1975).
[16] M. Chemtob and B. Desplanques, Nucl. Phys. **B78**, 139 (1974).
[17] R. B. Wiringa, V. G. J. Stoks, and R. Schiavilla, Phys. Rev. C **51**, 38 (1995).
[18] M. Simonius, Phys. Lett. **B41**, 415 (1972).
[19] M. Simonius, Nucl. Phys. **A220**, 269 (1974).
[20] R. Schiavilla, J. Carlson, and M. Paris, Phys. Rev. C **70**, 044007 (2004).
[21] R. Machleidt, Phys. Rev. C **63**, 024001 (2001).
[22] G. A. Miller, Phys. Rev. C **67**, 042501(R) (2003).
[23] W. C. Haxton, C.-P. Liu, and M. J. Ramsey-Musolf, Phys. Rev. Lett. **86**, 5247 (2001); Phys. Rev. C **65**, 045502 (2002).
[24] C.-P. Liu, C. H. Hyun, and B. Desplanques, Phys. Rev. C **68**, 045501 (2003).
[25] C.-P. Liu, C. H. Hyun, and B. Desplanques, Phys. Rev. C **69**, 065502 (2004).
[26] J. W. Durso *et al*., Nucl. Phys. **A278**, 445 (1977).
[27] R. Machleidt, K. Holinde, and C. Elster, Phys. Rep. **149**, 1 (1987).
[28] S.-L. Zhu, S. J. Puglia, B. R. Holstein, and M. J. Ramsey-Musolf, Phys. Rev. D **62**, 033008 (2000).
[29] M. J. Iqbal and J. A. Niskanen, Phys. Rev. C **49**, 355 (1994).
[30] G. S. Danilov, Phys. Lett. **18**, 40 (1965).
[31] B. Desplanques and J. Missimer, Nucl. Phys. **A300**, 286 (1978).
[32] S.-L. Zhu *et al*., Nucl. Phys. **A748**, 435 (2005).